Model TUCS1000-
Targeted Ultraviolet Chemical Sensor

Targeted Ultraviolet Chemical Sensors (TUCS) are in-situ, non-contact, non-invasive, non-destructive sensors that require no sample handling or preparation. They employ UV laser induced native fluorescence and resonance Raman spectroscopy to detect and classify unknown molecules and molecular structures. By employing deep UV excitation wavelengths the need for tagging target materials with dyes is eliminated. Dye tags are a significant source of error in many measurements and can obscure the chemistry being measured. Using excitation wavelengths below 250nm, native or endogenous fluorescence and UV Raman emission of target molecules can be measured simultaneously without mutual interference. The Raman analyzer portion of the instrument is not presently available.

Sensitivity and Specificity
Fluorescence Limit of Detection of this sensor is as low as one microorganism at a working distance of 45cm or 100 TRP molecules at a distance of 4cm. Other organic molecules such as BTEX have sensitivity in the PPT range. Resonance Raman sensitivity is about 1000 times lower. Specificity will be discussed later.

Applications:
TUCS are designed to be employed as sensitive, in situ, autonomous, industrial or environmental monitors. The sensors developed by Photon Systems operate in the deep ultraviolet to enhance their sensitivity and specificity in identifying certain molecular structures such as organic molecules and well as other molecules that are optimally excited in the UV to emit fluorescence and Raman.

Typical applications for TUCS instruments include in situ, real time measurement and characterization:
- Homeland security detectors for biological and chemical weapons materials;
- Ultrasensitive organic surface contamination detection in high quality optical fabrication, operating room surface inspection, etc.
- Cleaning validation for ultra-sensitive reagent applications
- Water quality in waste treatment plants where the content of nitrates, nitrites, carbonates, aluminates, and other water quality contaminants need to be measured on a regular basis;
- Well water or ocean water quality: sea farming, well water testing, domestic water quality;
- Chemical and microbial detection and identification in water, air and or surfaces
- Quality measurement of synthetic chemical vapor deposited diamond and diamond like carbon films in hard disc drive, super abrasives manufacturing, and other synthetic diamond applications;
- Quality measurement of epitaxial films employed in microelectronics manufacturing; substrate surface quality.
- Quality measurement of the surface condition, chemistry and quality of other elements of microelectronic devices;
- General measurement of targeted chemical compositions in quality control measurements in manufacturing such as adhesives, plastics, organic chemicals, etc

Specification:

Self-contained deep UV Chemical Sensor containing:

- High power deep UV laser with power supply and digital controller capable of data sampling rates to 30 Hz.
- Spectral isolation filter for excitation wavelength
- Laser excitation power reference detector
- 6 high gain miniature PMT detection channels used to simultaneously detect a combination of laser induced native fluorescence and Raman emissions.
- A choice of number of fluorescence detection channels with selectable band center, bandwidth and slope matched to the chemical environment of the sensor.
- 7 channel PMT controller with digital gated boxcar integrator and averager containing 64MIP microprocessor with 256K RAM and 256K flash memory.
- Power: 5W standby, 6W full power – can be operated by battery or solar cell array.
- Voltage: 24VDC from battery or line source
- Size: 6" x 4" x 14"
- Weight: 12 lbs
- Control: Ethernet, IEEE485, or RF
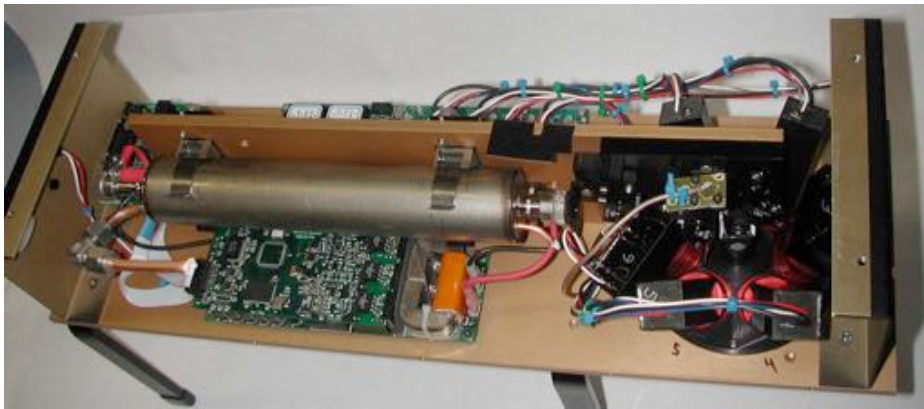- Software: Labview VI operated from PDA or other computer

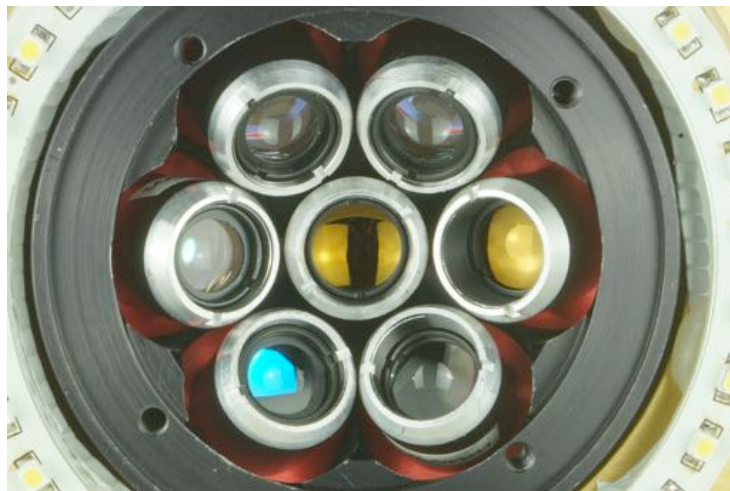*Figure 1. Internal Photo of Targeted UV Chemical Sensor*

Figure 2. Photo of 6 Channel Detection Aperture
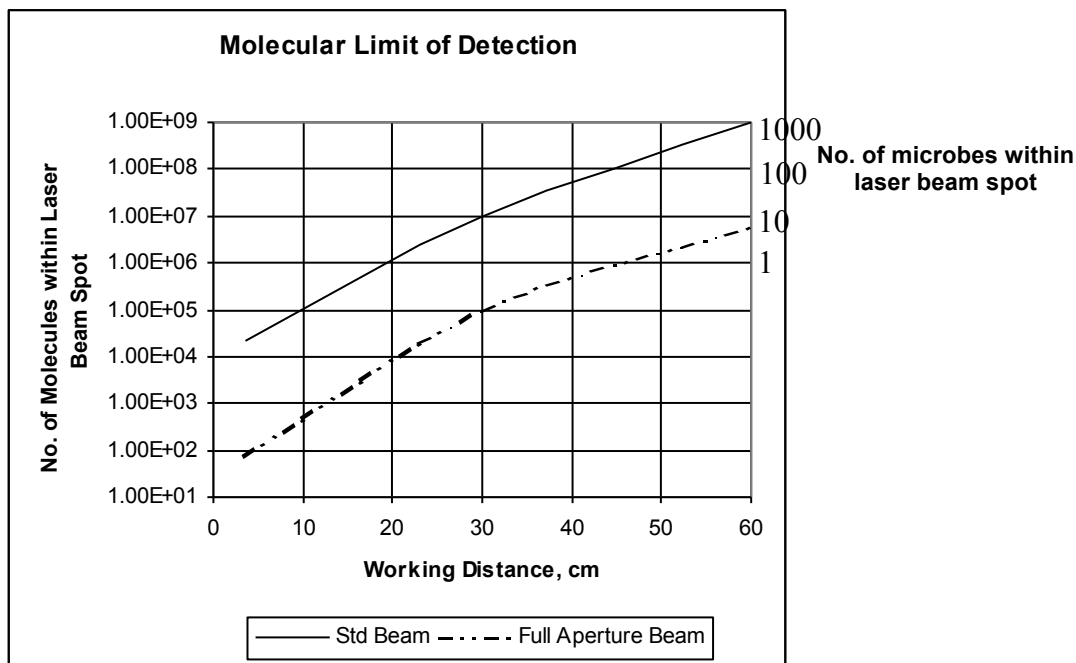
Molecular Limit of Detection

Figure 3. Fluorescence Limit of Detection (FLOD) for tryptophane molecules and whole microorganisms versus Working Distance

Background on UV laser induced resonance Raman and resonance fluorescence

High levels of chemical specificity can be obtained using Raman spectroscopy without sample preparation, contact, or destruction[1]. Raman scattering is, in general, a very inefficient process. Normal Raman scatter cross-sections are about 10^{-26} cm^2 for a major Raman line (1615 cm^{-1}) of a typical microorganism[2]. Normal Raman occurs when the excitation wavelength is far from an electronic absorption band of the material. If the excitation wavelength is within a major electronic absorption band associated with the 1615 cm^{-1} Raman band, the scattering signal is "resonance" enhanced by as much as eight (8) orders or magnitude, such that the scatter cross-section improves to about 10^{-18} cm^2. In contrast, maximum resonance (native) fluorescence cross-sections for the same microorganism, measured over a 30nm wide bandwidth near the peak of fluorescence, are about 10^{-11} cm^2. This is a factor of 10^7 improvement over resonance Raman and clearly demonstrates the sensitivity of resonance fluorescence compared to resonance Raman. However, much higher levels of specificity can be obtained with Raman.

Resonance bands for nucleic and aromatic amino acids occur in the deep UV between about 220nm and 280nm. When excited at wavelengths less than 250nm, Raman scattering occurs within about 20nm to 30nm above the excitation wavelength,

---

[1] Cary, P.R. (1982) *Biological applications of Raman and resonance Raman spectroscopies*, Academic Press, New York.

[2] Wilfred Nelson, U.Rhode Island, private communications.

corresponding to about 4000 cm^{-1}. Fluorescence occurs only above about 280nm, independent of excitation wavelength. Between the excitation wavelength at about 280nm, there exists a fluorescence-free region in which to observe the weak Raman scattering signal. A Raman shift of 4000 cm^{-1} corresponds to a wavelength of 247nm when excited at 225nm, 278nm when excited at 250nm and 298nm when excited at 266nm. It is therefore ideal to combine UV resonance fluorescence and resonance Raman spectroscopy to form an integrated tool for both detection and identification of biological agents since they offer a great combination of sensitivity and specificity that do not share overlapping observation wavebands.

Although resonance fluorescence is not the specific subject of this program, it is an integral part of the overall detection method and is closely tied to the excitation wavelengths used for resonance Raman excitation. Therefore we will include a brief discussion of resonance fluorescence here also.

UV Resonance Fluorescence Detection of Biological Agents

All microorganisms require continual input of free energy through cellular metabolism. The source of this energy input is electrochemical potential between electron donors and acceptors. The primary carrier of free energy is adenosine triphosphate (ATP), which is derived from the oxidation of fuel molecules such as carbohydrates and fatty acids. Typical molecules responsible for the transport of energy within cells are porphyrins, quinones, flavins, NADH, etc. Other essential building blocks of living organisms are nucleic acids, amino acids and peptides, sugars and lipids, and polysaccharides. Most of these organic molecules contain chromophores which, when excited at an appropriate wavelength, will provide a signature of the material and give a good indication of the general class to which the microorganism or organic material belongs. Many other organic and inorganic materials also fluoresce that are not harmful to humans. However, when the excitation and emission wavebands are carefully chosen, these can be discriminated against with high reliability.

Optimum Fluorescence Excitation and Observation Wavelengths

Resonance fluorescence of biological agents is likely the only technique sufficiently sensitive to discover, *in situ* without any sample preparation, the presence and rough classification of a single or few numbers of microorganisms. It is the only viable method of performing non-contact biological classification of aerosols in situ[3] because of the small dwell time for observation in an aerosol stream.

---

[3] Faris, G.W., R.A. Copeland, K. Mortelmans, and B.V.Bronk, "Spectrally resolved absolute fluorescence cross sections for bacillus spores", App.Opt.,Vol.36, No.4, pp.958-967, 1 February 1997.
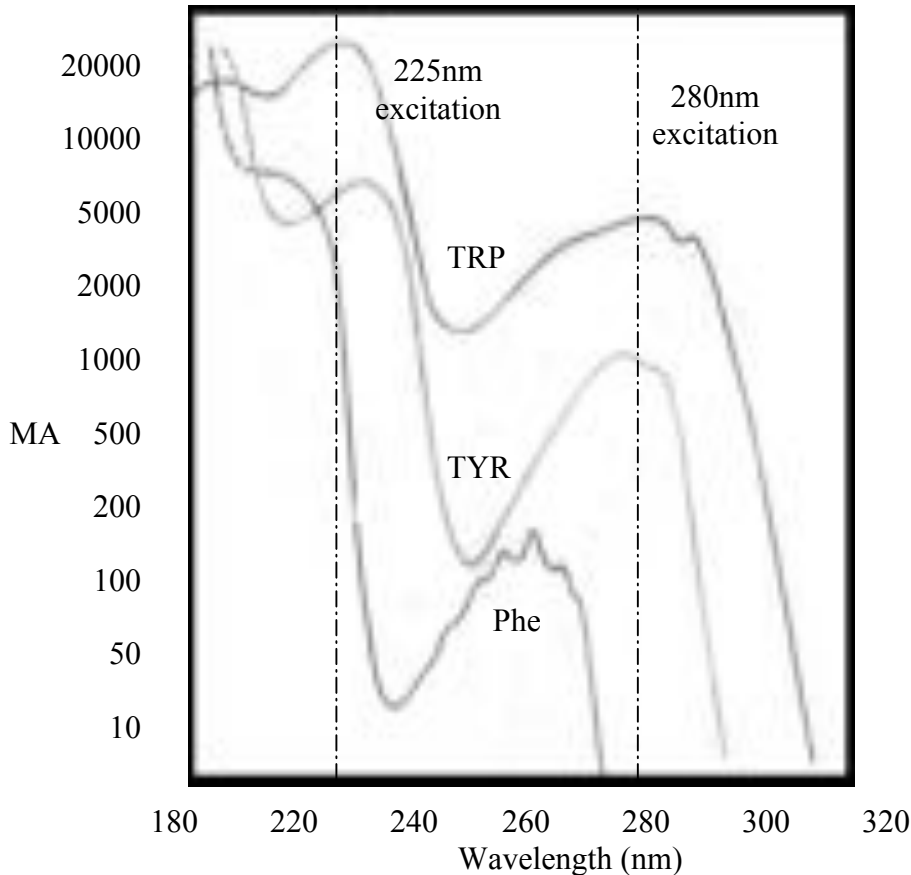
Figure 4. Molar Absorptivity of aromatic amino acids

Fluorescence emission always occurs at wavelengths longer than the excitation wavelength. Fluorescence cross-sections are a function of both the emission and excitation wavelength. If excitation occurs outside of an absorption band, the cross-section will be low, no matter how low the excitation wavelength. It is possible to select an excitation wavelength to emphasize the contrast or targeted biological agents against a wide array of potential background materials. The fluorescence spectrum of a molecule is generally a mirror image of its absorption spectrum and usually forms in broad bands, dependent on the vibrational, rotational and electronic energy level structure of the atom or molecule and its surroundings.

Figure 4 shows the molar absorptivity of the major aromatic amino acids[4]. Note that the molar absorptivity peaks for Trp about 225nm and for Tyr about 230nm. Trp absorption at 225nm is 5 to 10 times stronger than in the traditional excitation wavelength at 280nm. The fluorescence cross-section and related efficiency is similarly higher when excited near their optima. It is a common notion that excitation at shorter wavelengths causes more interference with background materials. This is incorrect as will be shown below. The fluorescence cross-section and subsequent emission intensity is a function of both excitation and emission wavelength. This is illustrated in the following Excitation-Emission-Matrix (EEM) diagrams. EEM diagrams display the fluorescence intensity or cross-section as a function of both excitation and emission wavelength with the iso-

---

[4] Thomas E. Creighton, **Proteins, Structures and Molecular Properties**, (W.H. Freeman and Company, New York, 1993)

intensity shown as contour lines, as illustrated below in Fig. 5 for Bacillus subtilis in both the vegetative and spore form.

It is important to note that both the spores the vegetative cells have two optimum excitation wavelengths, one near 230nm and one near 280nm. Emission maxima vegetative cells at both excitation wavelengths are the same, at about 330nm, as expected. The EEM diagram for Bacillus subtilis in spore form (@10^4 per ml) is also shown in Fig. 2. Optimum excitation wavelengths are essentially the same for B .subtilis spores and vegetative cell. However, the optimum emission wavelength for spores is close to 305nm compared to 340nm for vegetative cells. This is a clearly distinguishable marker feature of spores.

Driks[5] shows that the spore coat for B. subtilis is dominated by tyrosine, whose fluorescence signature peaks near 300nm rather than the tryptophan, whose peak is near 350nm. This is shown by comparison with the TRP and TYR EEM diagrams shown below the B. subtilis in Fig. 2 above. A secondary optima occurring at Ex=280nm and EM=400nm is a result of a denatured alcohol contaminant in the sample. Below in Fig. 3 are the EEM diagrams of several common background materials and minerals. From the above EEM diagrams it is evident that B.subtilis vegetative cell fluorescence occurs at shorter wavelengths than pure Trp and long wavelengths than pure Tyr. The spore form is very closely related to Tyr as described by Driks.

The EEM diagrams in Fig. 6, below, illustrate the broad variation of fluorescence fingerprints of many common materials. Most materials exhibit one to three fluorescence peaks. Paper has strong peaks in the blue/green due to doping of paper with fluorescent dyes to enhance "whiteness". The EEM fingerprints of any of these materials are significantly different from B. subtilis in either the spore or vegetative form. However, when detection is accomplished using a single excitation wavelength, some similarities do exist.

---

[5] Driks, A., "Bacillus subtilis spore coat", Microbiology and Molecular Biology Reviews, Vol.63, No.1, pp.1-20, Mar. 1999.
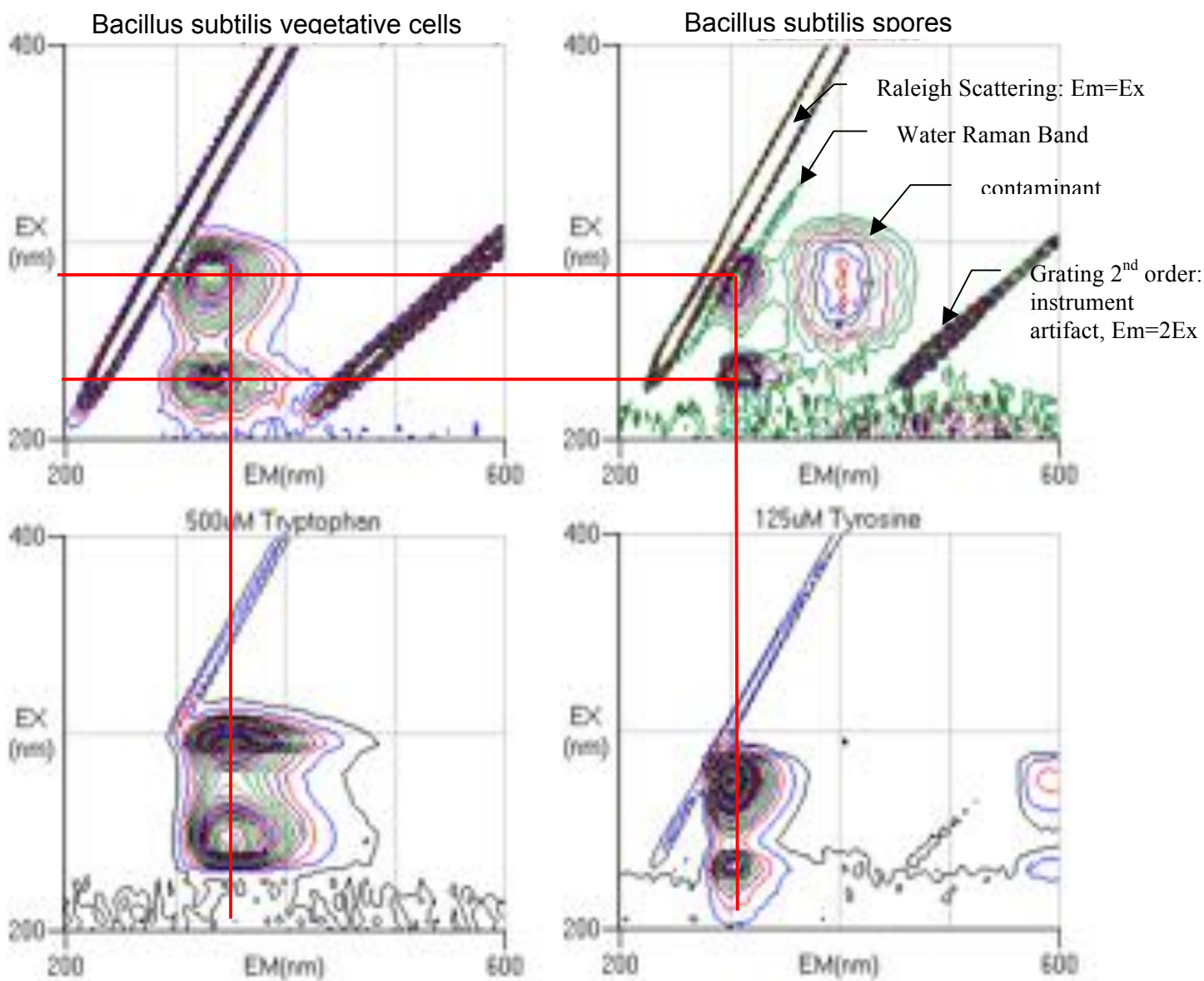
Figure 5. EEM diagrams of B.subtilis in spore and vegetative form with Trp and Tyr EEM diagrams

When excited near 280nm, the emission spectrum of several plastics is similar to B. subtilis. However, when excited near 230nm, the spectrum is distinctly different. What is of interest is to select an excitation wavelength and a set of emission observation wavelengths for which biological agents have the highest possible differential fluorescence against the widest range of background materials. It is clear from the above data that deeper UV excitation wavelengths do not "excite everything" as is commonly suggested.
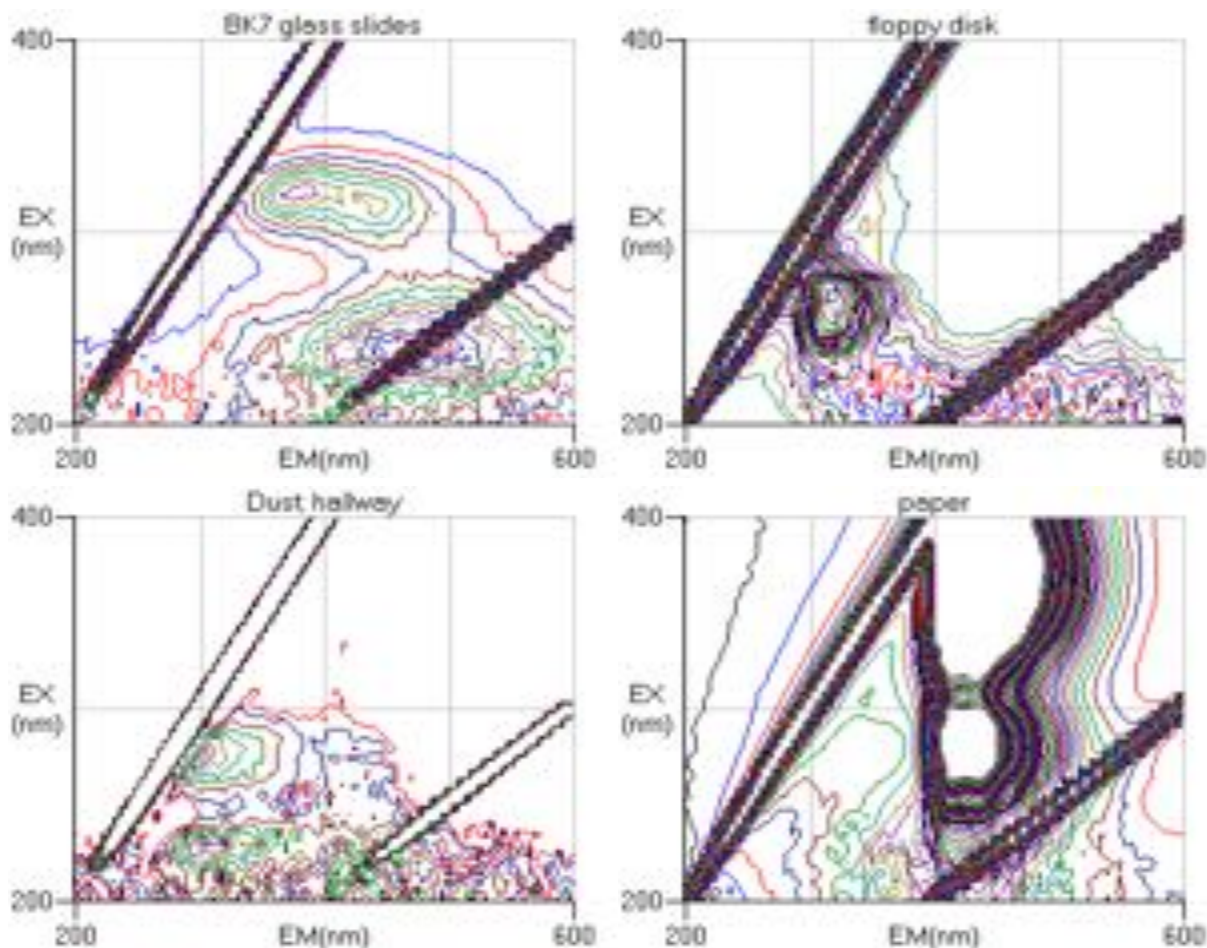
Figure 6. EEM diagrams for sample background materials

Although fluorescence is not known for its chemical specificity, by choice of the number of spectral detection bands and their bandwidth and band location, a significant level of chemical specificity can be achieved. Six detection bands are used in our TUCS instrument. We can alter these bands but the following selection is a good example of what level of specificity is achievable.

It is a common notion that excitation at shorter wavelengths causes more interference with background materials. This is incorrect since each material has a unique fingerprint with fluorescence cross-section and subsequent emission intensity dependent on both excitation and emission wavelength, as illustrated in figures 1 and 2 as well as over 100 other EEM diagrams obtained for a wide range of materials listed in the next page. Fluorescence of most materials normally occurs between about 270nm and 700nm. Fluorescence at the shorter end of this wavelength range results from molecules that have single phenyl rings while fluorescence at the longer end results from molecules that have several phenyl or benzene rings, such as polyaromatic hydrocarbons. Most fluorescent materials exhibit one to three fluorescence peaks. Minerals typically have only one.
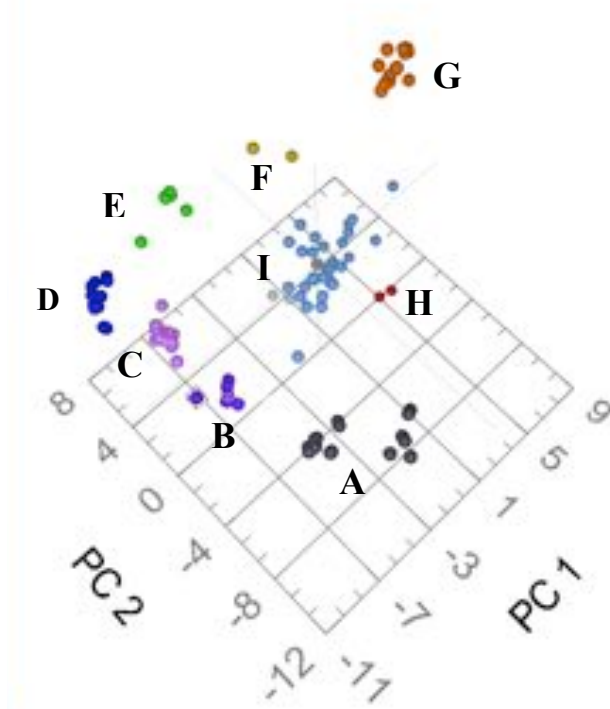
Figure 7. Illustration of differentiability of biological, organic and other compounds and particles based on deep UV laser induced native fluorescence at 235nm

In order to detect and differentiate a set of target materials with a high degree of fidelity against a wide range of background materials it is important first to chose the optimum excitation wavelength. Target materials include bacterial spores, vegetative cells, or biological residue materials such as aromatic amino acids, peptides or proteins, or nucleic acids, virus', etc. Background materials can include household materials, organic solvents, polyaromatic amino acids (PAH's), minerals, etc. The EEM fingerprint of most background materials is significantly different from a biological cell in either the spore or vegetative form. But even when a signature is similar, it is rarely similar enough that it cannot be differentiated, depending on the resolution of the spectrum obtained.

High-resolution excitation-emission matrix (EEM) data sets of over 100 pure samples were obtained using a Hitachi F4500 spectrofluorimeter where excitation ranged from 200nm to 400nm and emission ranged from 200nm to 600nm. These samples form the initial "training set" used with principal component analysis (PCA) and support vector machines (SVM) to optimize the ability to identify materials. Examples of these data sets are shown in Figs. 5 and 6 above. At excitation wavelength intervals of 5nm the relationship between the native fluorescence spectra of all material samples was compared using principal component analysis (PCA), a linear multivariate analytical method. Figure 7 illustrates the ability to differentiate ten (10) groups (A through I) of samples excited at 235nm. Each group is made up of similar component materials that include organic and biological materials but which also include minerals and other materials as described below. Materials illustrated in Fig. 7 are grouped according to their general composition. **Group A** materials represent variants on single phenyl ring materials: phenylalanine, Gly-Phe-ala, Gly-phe-ser, xylene, tyrosine, toluene, dichlorobenzene, Glu-tyr-glu, Gly-tyr-gly, Leu-tyr-leu, Lys-tyr-lys, and n-acetyl-tyr-ethyl ester. **Group B** materials are bacterial spores of a variety of types including b. atropheus, b. pumilis, C. sporogenes (strain 1), C. sporogenes (strain 2), and G.

stearothermophilus. **Group C** materials are bacterial cells as well as lysates (supernatant and membrane fractions) including: S. oneidensis membrane, anaerobic S. oneidensis supernatent, S. oneidensis membrane, S. oneidensis supernatent, b.pumilus membrane, aerobically grown b.pumilus supernatant, b.pumilus whole cells, b.atropheus membrane, b.atropheus supernatant, b.atropheus whole cells, and S. oneidensis whole cells. **Group D** materials are two ring materials with or without R groups including 1,2 dimethnaph, 1,3 dimethnaphthalene, 1,4 dimethnaphthalene, 1-ethyl naphthalene, acenaphthene, and dibenzothiophene. **Group E** are indoles including tryptophan, glu-trp-glu, lys-trp-lys, carbazole, and indole. **Group F** materials are 3 ring materials with bent conformation such as phenanthrene and phenanthroline. **Group G** include folded 4 ring and straight 3 ring materials including pyrene, methylanthracene, methylpyrene and anthracene. **Group H** includes 5 ring and larger ringed organics including perylene, NADH, riboflavin, and fluoranthene. **Group I** materials are pollens, common household materials, and other contaminants including: marigold pollen, yellow hibiscus pollen, mechanical pencil lead, drywall, corn starch, crayola chalk, ceiling tile, Sweet-n-low, and Splenda.

Figure 7 clearly illustrates that a wide range of biological, organic and other chemical composites can be differentiated with a fairly high level of accuracy. Typically the ability to repeat the position of a chemical identity with repeated measurements is less than the size of a data point sphere in Fig. 7. Microbial spores and vegetative cells are clearly differentiable from each other as well as all of the other chemical groups. Even within the spore group bacillus and clostridium species are differentiable. Similarly vegetative cells grown aerobical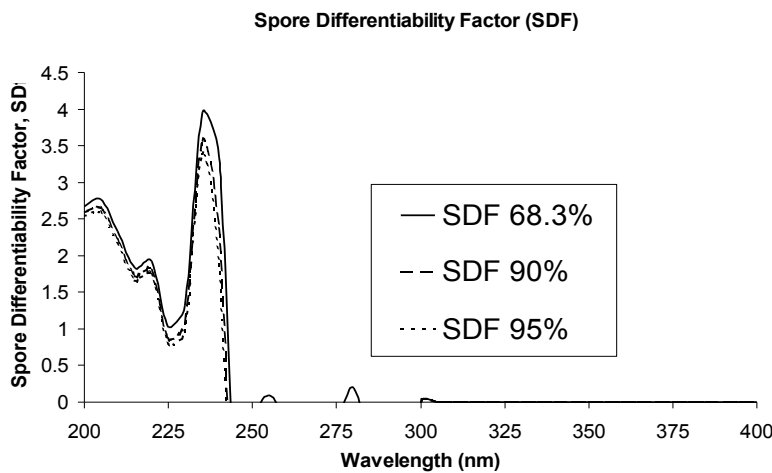ly and anaerobically are clearly differentiable. In addition, background materials such as household materials, volatile organic hydrocarbons, and other materials are very clearly differentiable from spores. Training of the algorithm is possible in order to better differentiate materials not in the training set used in the above example.

Figure 8. *Spore Differentiability Factor, SD$_f$, for 10 groups of samples*

To quantify the ability to differentiate groups of materials the 3D PCA centroid and spherical standard deviation of each group was determined. Using a spherical standard deviation should be very conservative since all materials except household contaminants lie close to a line and are not distributed in a spherically symmetric cluster. Spore differentiability factor, SD$_f$, is the distance between the centroid of the spore group and any other material, minus "n" times the standard deviation of the spore group. The

ability to differentiate between groups or individual materials is dependent on several factors including excitation wavelength, spectral resolution, and the number, bandwidth, and location of detection wavebands in sensors employing non-contiguous detection wavebands. Figure 4 shows SD_f as a function of wavelength for three confidence levels, corresponding to n = 1, 1.645, and 1.96 times the standard deviation. Confidence levels for spore identification are not directly related to false alarm rate since SD_f is defined as the distance to the closest interferant and NOT the most likely interferant. Figure 4 shows that the ideal excitation wavelength for spore discrimination is against all background interferants is 235nm. At present there are no miniature lasers emitting at this wavelength, although Photon Systems has lasers at this wavelength under development. The 224nm laser used in this instrument is able to differentiate spores with over 99% confidence. No laser with excitation wavelength above about 240nm can perform as well.

Figure 8 shows the differentiability factor versus the number of detection bands for contiguous bands (diamonds) and non-contiguous bands (circles). The differentiability data of Fig. 7 are based on data with a spectral resolution of 2nm over a range from 280nm to 500nm. Fig. 9 illustrates that the ability to differentiate spores decreases with the number of contiguous (adjacent) detection bands. Significantly better differentiability can be achieved with fewer numbers of detection bands if the bands are non-contiguous and are located to optimize the targeted group of materials, which in this case are spores. It is possible to achieve the same differentiability with 5 or 6 non-contiguous bands as with 100 contiguous bands when the concentration of the band centers is located in the deep UV between 270nm and 350nm.

Since the sensitivity of detection is proportional to the bandwidth of each detection band, fewer numbers of detection bands improves sensitivity. Optimizing the ability to detect and identify spores depends on the product of the spore differentiability factor and bandwidth.
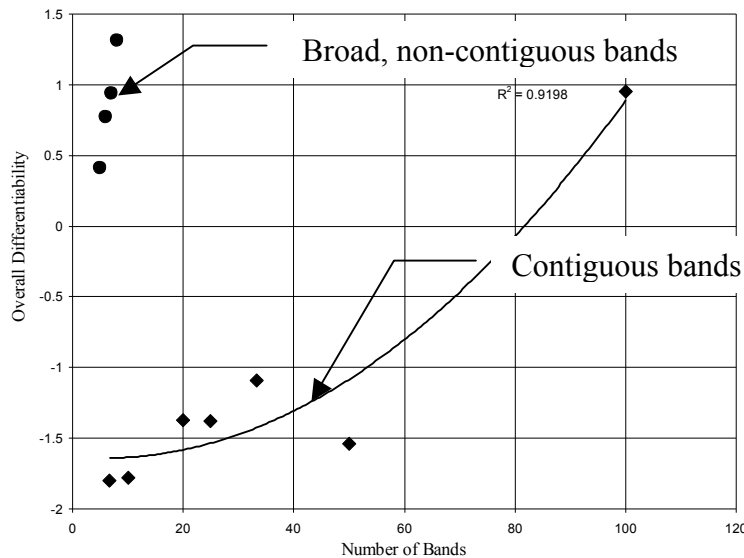
Figure 9. Effect of spectral resolution and band selection on differentiability

UV Resonance Raman Identification of Biological Agents

Over the past ten years UV resonance Raman spectroscopy has been increasingly used for detection and identification of microorganisms and study of cellular function[678910]. UV resonance Raman spectroscopy allow the measurement of clear band structures within the electronic absorption manifold of the target biological molecules and thereby enables the ability to more clearly characterize unknown biological materials. Photon Systems has benefited from close collaborations and association with Professors Sanford Asher of the University of Pittsburgh and Wilfred Nelson of the University of Rhode Island in conjunction with our development of deep UV lasers and miniature Raman instruments. Both of these men are known for their groundbreaking work in UV resonance Raman spectroscopy, especially as it applies to characterization of organic molecules and the molecules of life. We recently published a paper with Prof. Asher[11].

It has been clear for several years that unique ultraviolet resonance Raman spectral signatures can reliably be detected in as few as 20 bacterial cells with low power consumption and low photon flux levels (Nelson, 1993[12]; Nelson, et.al[13], 1993; Chadha, et.al., 1993[14]). In fact, UVRR has made possible the detection and characterization of single cells.

Taxonomic Raman Marker Bands

A summary of the major taxonomic marker bands of highly degenerate functional groups occurring within microorganisms is shown below in Table I.

Table I. Major Taxonomic Raman marker bands for biological agents

Material	Raman Band Locations						
Tryptophan	753	879 **1011**		1353		**1555**	1615
Tyrosine		831 852	**1180** 1210				**1615**
Guanine				1320 1365	**1485**	1577 1603	
Adenine				**1337**	**1485**	1580	
Cytosine					**1530**		
Dipicolinic Acid			**1017** **1195**	**1396** 1446			

Identification of biopolymers or organisms using UV Raman spectroscopy depends on the ability to produce interpretable, reproducible spectra. DNA and cell surface antigens

---

[6]W.H.Nelson, R. Manoharan and J.F. Sperry, "UV Resonance Raman Studies of Bacteria", App. Spect. Reviews, 27 (1), pp67-124, 1992

[7] S. Chadha, W. H. Nelson and J.F. Sperry, "Ultraviolet micro-Raman spectrograph for the detection of small numbers of bacterial cells", Rev. Sci. Instrum. 64 (11), pp.3088-3093, Nov. 1993

[8] Z. Chi and S. A. Asher, "UV resonance Raman Determination of Protein Acid Denaturation", Biochemistry, 37, pp.2865-2872, 1998.

[9] N.Cho and S.A. Asher, "UV resonance Raman studies of DNA-Pyrene interactions", J.Am. Chem.Soc. 115, pp.6349-6356, 1993

[10] F. Sureau, et.al., "An ultraviolet micro-Raman spectrometer: Resonance Raman spectroscopy within a single cell", App.Spect., 44, No.6, pp.1047-1051, 1990

[11] Sparrow, M.C., J.F. Jackovitz, C.H. Munro, W.F. Hug, and S.A. Asher, "A New 224nm Hollow Cathode UV Laser Raman Spectrometer", *J. App. Spectroscopy*, Vol. 55, No. 1, Jan 2001.

[12] Nelson, W.H. (1993) *Rev Sci. Inst.* (11):3088-3093

[13] Nelson, W.H. , Manoharan, R., and Sperry, J.F. (1992) *Appl. Spect. Rev.* 27(1), 67

[14] Chadha, S., Nelson, W.H., Sperry, J.F. (1993) *Rev. Sci. Inst.* (11):3088-3093

are the most attractive targets as potential markers for cellular or bacterial identification. Identification of organisms using UV Raman spectroscopy has focused on the ratio of a few taxonomic marker bands (Ref.13). These band markers are based on ratios of tryptophan and tyrosine and DNA base pairs that can be characteristic of an organism. As mentioned previously, most biological materials have repeating functional groups that are highly degenerate. These include nucleic acid base pairs and aromatic amino acids. These repeating units have Raman spectra that are very similar to the spectra of the monomers upon which they are based. Raman spectra of B. cereus in several forms is shown below in Fig. 10 in using 242nm excitation: vegetative, spore and germinated spore (Ref.13). Major Raman marker bands are shown at 1019 cm^{-1}, 1485 cm^{-1}, 1530 cm^{-1}, 1555 cm^{-1}, and 1615 cm^{-1}. The measurement bandwidth illustrated is about 25 cm^{-1}.

Bacteria can be characterized as Gram positive versus Gram negative based on the 1555 cm^{-1}/1615 cm^{-1} intensity ratio. Gram negative bacteria have a much higher ratio of the tryptophan intensity at 1011 cm^{-1} or 1555 cm^{-1} compared to the Tyr + Trp intensity at 1615 cm^{-1}. In general, this ratio is described as the intensity in broad spectral regions centered near the 1555 cm^{-1} and 1615 cm^{-1} Raman bands. However, the exact position, center of gravity, band width, and other features of each band can provide more detailed identification of bacteria. However, the relationships are presently unknown. It is believed that these marker bands primarily describe the surface composition of an organism.
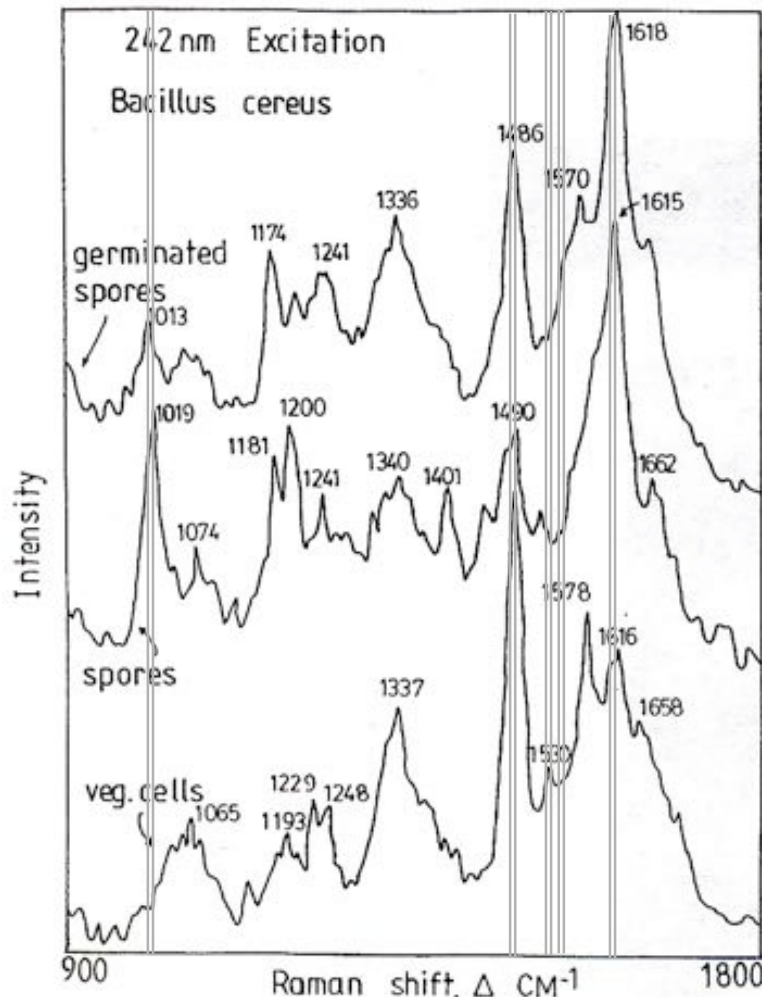

Figure 10. Resonance Raman spectra of B. cereus in various

Within Gram positive organisms such as spores, or vegetative cells there is further sub-classification G+C percentage. This is determined by the 1530 cm^{-1}/1485 cm^{-1} Raman band intensity ratio. The intensity of the 1485 cm^{-1} peak is taken as closely proportional to the total amount of nucleic acid on a molar basis (DNA + RNA) in the cell.   The intensity of the peak at 1530 cm^{-1} can be assumed to be proportional to the moles of cytosine in the nucleic acids. It follows that the mole fraction of G+C in the bacteria should be proportional to the ratio of the 1530 cm^{-1} and 1485 cm^{-1} peaks.

Following is a graph of the 1530/1485 cm^{-1} ratio versus the known percentage of G+C of DNA in 14 different bacterial species grown on TSA and in TSB, respectively (Ref.13). The peak intensity ratios versus molar percent G+C are linear dependent, as shown in Fig. 11.
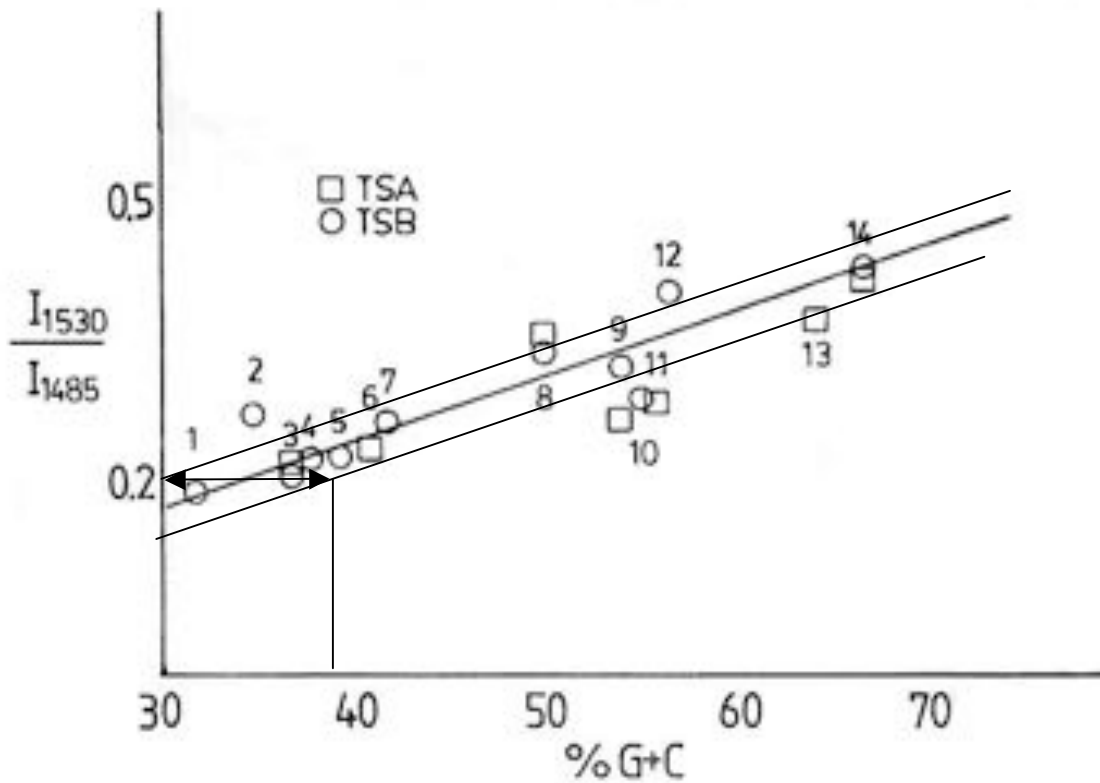

Figure 11. Plot of 1530 cm^{-1}/1485 cm^{-1} versus known G+C for 14 bacterial species. 242nm excitation. (Adapted from Ref.13)

Three lines are shown in Fig. 11 which represent the mean and ± one standard deviation of the data. This preliminary estimate illustrates the potential to identify an organism within about ± 3 to ± 5 mole percent G+C. In combination with identification of the Gram polarity and whether the organism is a spore, the G+C content can provide significant specificity in identification or biological agents. The organisms employed in Fig. 11 are tabulated below in Table II.

Table II. DNA mole fraction for Guanine + Cytosine for bacteria in Fig. 8

Plot No.	Organism	Mole% G+C	Gram	Spores	Virulence class[g]
	Clostridium botulinium	28.2[i]	+	X	2
	Rickettsia prowasecki	28.9[i]	-		3
	Staphylococcus aureus	32.8[b]	+		2
1	Bacillus cereus	32[a]	+	X	1
2	Enterococcus faecalis	34-36[a] 37.5[b]	-		1
	Staphylococcus simulans	34-38[a]	+		1
	Bacillus antracis Ames	35.2[b]	+	X	2
	Streptococcus agalactiae	35.5[b]	+		1
4	Proteus vulgaris	36-40[a]	-		1
3	Bacillus magaterium	37[a]	+	X	1
5	Proteus mirabilis	39.5[a]	-		1
6	Bacillus subtilis	41[a]	+	X	1
7	Acinetobacter calcoaceticus	42[a]	-		2
	Bacillus subtilis	43.5[b]	+	X	1
	Shewanella oneidensis MR1	45.9[b]	-		1
	Yersinia pestis.	47.6[i]	-		3
	Vibrio cholerae	47.6[i]	-		3
8	Escherichia coli, K12-MG1655	50.7[b]	-		2
	Shigella dysenteriae	50[i]	-		2
	Samonella tphi	52.1[i]	-		2
9	Enterobacter aeroqenes	54.3[a]	-		1
10	Alcaliqenes faecalis	54.8[a]	-		1
11	Enterobacter cloacae	55.4[a] 57.2[b]	-		1
12	Aeromonas hydraphila	55.7[a]	-		1
	Brucella suis 1330	57.2[b]	-		3
	Brucella melitensis	57.2[c]	-		3
	Aeromonas hydrophila	59-62[c]	-		1
	Pseudomonas putida	61.4	-		1
13	Pseudomonas aeruqinosa	64[a],66.4[b]	-		1
14	Micrococcus luteus	66.3[a]	+		1
	Alcaligenes faecalis	66.7-69.9[c]	-		1
	Burkholderia pseudomallei	68.06[i]	-		3
a=A.I.Laskin & H.A.Lechevallier(eds), CRC Handbook of Microbiology, Vol.II, CRS Press, Cleveland, 1973. b=tigr, i=Sanger Inst.					

Biological Agent Identification Specificity

One possible detection and identification strategy for biological agents using laser induced resonance fluorescence and UV Raman spectroscopy is as follows:

a.   Determine if a particle is biological or non-biological based on laser induced resonance fluorescence measured in the 300nm region.

b.   If particle is biological, measure the relative UV Raman intensity at five (5) Raman bands centered at 1017 cm^{-1}, 1485 cm^{-1}, 1530 cm^{-1}, 1555 cm^{-1} and 1615 cm^{-1}.

c.   Determine if the particle is Gram positive or negative based 1555 cm^{-1} /1615 cm^{-1} ratio.

d.   Determine if the particle is a spore based on the 1017 cm^{-1} /1615 cm^{-1} ratio.

e.   Determine the GC% based on the 1530 cm^{-1} /1485 cm^{-1} ratio.

Measurement of the Raman scattering in only five (5) broad ($\approx$40cm^{-1}) bands ***provides knowledge of the: Gram polarity; form of organism; and G+C percent***. These measurements can be made rapidly and correlated using any of several artificial neural net or PCA/PCO algorithms to give a relatively high degree of confidence in identifying organisms within a narrow range.   These measurements could be made in sub-second time scales and possibly as short as a millisecond or faster.

Using this fast and simple 5-band Raman technique, it would appear that it is unlikely this method would be able to specifically differentiate B. antracis against a background containing a wide range of other similar spore interferants since the detection accuracy corresponds to only about ± 4 % in G+C concentration. The closest spore to B. antracis at GC=35.2% is B. cereus at 32% (Δ=3.2%) and B. magaterium at 37% (Δ=1.8%).   All three are spore formers and all are Gram positive. So none of the discriminators would have differentiated between these organisms with a low false alarm rate. However, this fast method will probably enable discrimination of B.subtilis from B.antracis. In addition, this method would be able to discriminate anthrax from a wide range of other bacterial spores and other microorganisms and identify them within a small range.

There are many UV Raman spectroscopic options that have yet to be evaluated to reduce the false alarm rate in identifying B. antracis or other virulent microorganisms.   The fast and simple approach described above does not take advantage of the much larger wealth of information contained in UV Raman spectra. Substantial differences in taxonomic marker band intensity, peak position, center of gravity, and band shape occur for each of the basic Raman marker bands. These are a result of environmental and conformational differences between organisms as well as more subtle compositional differences. In addition, there are other Raman marker bands that are clearly measurable which may give further discrimination to microorganism identification. In order to provide a higher level of biological agent specificity, higher resolution Raman spectra would be required. A reasonably way to triage a target would be to follow the laser induced resonance fluorescence and broadband UV resonance Raman with high resolution UV resonance Raman. Each of these techniques is successively more time consuming, less sensitive and more specific. At present there is no clear model to provide higher specificity based on more subtle nuances of the Raman spectra such as peak position or center of gravity variations due to difference is microorganisms….but we're working on it.